Clinical use of optical coherence tomography to evaluate the integrity of dental restorations

Cláudia C. B. O. Mota [1], Hannah U. K. S. Kashyap [2,3], Bernardo B. C. Kyotoku [3], Renata Cimões [1], John M. Girkin [4] and Anderson S. L. Gomes [1,3]

[1] Graduate Program in Dentistry. Universidade Federal de Pernambuco, Av. Professor Moraes Rego, 1235, Cidade Universitária 50670-901, Recife-PE, Brazil. Phone: 55-81-21268817 Fax: 55-81-21268836. E-mail: claudiabmota@gmail.com

[2] Photonova Inc, 110 Elm Crescent, Baie d'Urfé (QC) H9X 2P6, Canada.

[3] Department of Physics. Universidade Federal de Pernambuco, Av. Prof Luiz Freire, s/n, Cidade Universitária 50670-901, Recife, PE, Brazil. Phone: 55-81-21267636 Fax: 55-81-32710359. E-mail: anderson@df.ufpe.br

[4] Centre for Advanced Instrumentation, Department of Physics, South Road, Durham University, Durham, DH1 3LE, UK

Abstract

We have applied Optical Coherence Tomography (OCT) clinically to assess dental restorations in humans. Twenty patients with resin composite restorations in anterior teeth were selected and evaluated using a conventional radiographic examination, visual inspection and OCT. Images were obtained using a home built OCT system operating in the spectral domain, with an 850 nm superluminescent diode light source. The results were analyzed with respect to the integrity and marginal adaptation of the restoration. Using appropriate software failed and failing restorations, including those with lesioned regions, could be located prior to the placement of a new restoration. Lesions and failed restorations were identified with the OCT system that could not be seen by conventional visual and X-ray examinations and these were found to be present on surgical intervention. This *in vivo* study demonstrates that the OCT technique has a great potential to be used in clinical practice to assess dental restorations and prevent recurrent caries.

Keywords: Optical Coherence Tomography, Dental Diagnostics, Marginal Microleakage, Dental-Restoration Interface.

Introduction

In recent years, several methods using light have been proposed to address the need for better detection and diagnostic tools in dentistry. Digital imaging fibre-optic transillumination (DIFOTI), multi-photon imaging, quantitative light fluorescence (QLF), infrared fluorescence (DIAGNOdent), infrared thermography, Raman spectroscopy, optical coherence tomography (OCT) and terahertz imaging are a few techniques that are currently under evaluation for improved diagnosis [1-4].

Optical coherence tomography (OCT) is a recent, but well established low-coherence interferometric technique that allows the acquisition of high-resolution, non-invasive, cross-sectional images of biological tissue based on the detection of backscattered light [5,6].

OCT has already been applied *in vitro* and *in vivo* to a variety of medical specialties, including Ophthalmology [5], Dermatology [7], Gastroenterology [8], Cardiology [9] and Cellular Engineering [10].

The first study applying OCT to be carried out in Dentistry, both *in vitro* and *in vivo*, was in 1998, using a prototype handpiece for the characterization of both hard and soft dental tissues [11, 12]. In 2003, a commercial prototype OCT system was adapted to a commercial surgical microscope to perform *in vitro* and *in vivo* images of carious lesions and restorations [13]. OCT has also been employed for the early detection of oral cancer [14]. *In vitro* studies evaluating enamel interface restoration [15], early caries diagnostics [16], and analysis of the performance of dental materials [17] have also been reported. In 2006, the first OCT image of dental pulp was performed using rat's teeth [18]. Recently, remaining dentin and the pulp chamber from human teeth were also imaged by OCT *in vitro* as reported in [19]. Endodontic applications of OCT have been explored in order to evaluate root canals [20] and Sinescu and co-workers used OCT to investigate the marginal adaptation of fixed dental prosthesis before installing them in patients [21]. However, little work has been reported on OCT being used in a clinical setting as part of a clinical evaluation, specifically looking at restoration integrity.

Dental restorations provide a barrier restricting oral fluids and bacteria from entering the tooth after the removal of any damaged or missing tissue. An inadequate marginal seal can result in gap formation that leads to microleakage, which may be

responsible for marginal breakdown, recurrent caries, increased post-operative sensitivity, pulpal inflammation, and staining [22].

Microleakage, either from small or microscopic openings between the margins of the composite restoration and tooth is considered to be a major cause of restoration failure [23]. Microleakage can also result in bacteria penetrating the tooth-restoration space and into dentinal tubules, where secondary decay may occur and bacterial toxins will irritate the pulp. The oral environment, including occlusal forces and temperature variation, as well as the differences between the physical properties of teeth and restorative materials, polymerization shrinkage, the coefficient of thermal expansion, and modulus of elasticity can all contribute to microleakage. According to previous literature, if poor bond strength exists between the tooth and restorative material, a failure of adhesion may be caused by polymerization shrinkage, and microscopic gaps at the tooth-restoration interface can subsequently form [15, 22, 23].

The success of the restorative treatment depends on the integrity of the tooth-restoration interface and this particular region is the subject of much research and discussion in the Dental community. Clinically, the most common tools for detection of restorative failures are by tactile and/or visual inspection or by radiographic examination. However, since initial microleakages can be clinically and radiographically imperceptible, secondary caries may currently progress before the problem can be detected by the dental practitioner.

A recent study evaluating the enamel-restoration interface using OCT, in which just one patient was reported, has been published [24] and Negritu et al. [25] used OCT and confocal microscopy to investigate dental structures and restoration materials using extracted teeth.

Here we present an *in vivo* study employing a home built OCT system, operating in the spectral domain using a superluminescent diode at 850 nm, to detect failures at the enamel-dental restoration interface, and the integrity of superficial and internal structures of restorations in a clinical setting. This study was undertaken with 20 patients attending the Dentistry College of the Universidade Federal de Pernambuco. The relatively large number of attending patients allowed us to obtain and analyze the results in a very consistent manner. Results were compared to conventional radiographs and clinical examination, represented here by photographs.

Materials and Methods

This study was developed according to the guidelines given by Ethical Committee in Human Research of the Universidade Federal de Pernambuco, Brazil. Twenty patients with resin composite restorations in upper anterior teeth were selected. These patients were between 18 and 45 years old, both male and female, and had their restorations performed between 1999 and 2009. All the restorations had a superficial satisfactory clinical aspect with no obvious aesthetic failures such as staining, undesirable shape or obvious missing material.

OCT performs high-resolution, cross-sectional tomographic imaging of the internal microstructure in materials and biological systems by measuring backscattered or backreflected light. The intensity of the signal is a function of the scattering caused by the local changes in tissue structure of the tooth. Variations in scattering measured in relation to depth from a single point on the tooth surface are called an "A-scan". Taking several A-scans along a line produces information from a 'slice' of tooth tissue, which is the tomogram. The movement along the line of A-scans is known as the "B-scan" [1].

The key elements of an OCT system include a broadband light source, whose spectral width largely sets the axial spatial resolution; an interferometer, which generally employs a Michelson design, with one of the arms containing the sample and in the other arm, a delay line; and an optical detector, whose signal output is electronically treated and fed to a computer for the image generation. In the spectral domain (SD-OCT), there are no movable parts in the interferometer arms (except for lateral displacement of the beam on the sample), and the recombined beams from the interferometer are sent to a spectrometer and are Fourier analyzed [26].

The schematic diagram of the home-built OCT operating in the spectral domain, which was used in this study is shown in figure 1(a), and is the same as reported previously [19] where the full experimental details are described. The centre wavelength of the system was selected to be around 850 nm. Although longer wavelengths penetrate more deeply into the sample due to a lower scattering coefficient, this lower scattering coefficient also means a loss of sensitivity to slight changes in refractive indices. In order to maximize the sensitivity to changes we therefore opted for a shorter wavelength compared to the 1300 nm that reported previously [24, 25].

In summary, the output emission from a superluminescent diode (Broadband SLD Lightsource S840, SUPERLUM, Moscow, Russia) operating at 850 nm, with a spectral width of 49.9 nm and a fiber output power 25 mW was sent to a Michelson interferometer setup providing an axial resolution of 6 μm. In the reference arm a mirror was mounted on a piezoelectric base, whilst in the sample arm, a mirror controlled by a Galvanometer motor was used to scan the light on the sample. The reflected and back-scattered light coming from both arms was then recombined at the beam splitter and collected by a spectrometer.

[Fig. 1]

The maximum incident power on the sample was approximately 5 mW. The beam incident on the sample was focused using an achromatic 50 mm focal length (numerical aperture = 0.25) lens. For a typical beam diameter of 1 mm before the focusing lens, the lateral resolution was 54μm. The axial resolution is set, predominantly, by the bandwidth of the source, whereas the lateral resolution is determined by the numerical aperture of the final lens system. The lateral resolution is thus a compromise between the working distance and size of the final lens. To increase the lateral resolution one would shorten the working distance of the system, making it less useful for clinical applications, thus we opted for a lateral resolution of 54 microns and an acceptable working distance of around 50mm.

This optical delivery system was mounted on a 2D translation stage, though as the beam passes off a scanning galvo, this is used to scan either in the X or Y direction for data acquisition and only one axis of the translation stage was used for lateral movement of the imaging system. The control of the scanning systems was undertaken by a personal computer with a LabView based imaging program. A photograph of the entire system is shown in figure 1(b).

The signal produced by the spectrometer was also sent to the same computer which thus both controlled the scanning and data processing. The software generated an image into a fixed size screen (stored as a .png file) and a numeric array matrix (stored as a .dat file) containing the information about the A-scans and B-scan of each image, composed by 512 lines and 512 columns. As the LabView screen had a fixed size, the image file presented distortions along its longitudinal axis but provided the clinician with a real time image of the area under examination. The correctly sized image was obtained through subsequent manipulation of the .dat using the Image J software (NIH, USA). These processed images enabled the exact position of any restoration failure to

be seen clearly through the use of an appropriate colored look-up table and subsequently located and precisely measured.

To perform the OCT examination, a lip retractor was used on the patients, and their heads were positioned in an appropriate support, in front of the sample arm, seen in figures 1(b) and 1(c). The image acquisition time is less than one second (for each image, there was 0.1 second of pre-scan settling time and 80 μs of integration time) though the support was used to minimize movement which would otherwise blur the high optical resolution images. The authors analyzed the results with respect to the integrity and marginal adaptation of the restoration by visual inspection of the images in real time as well as on the images produced from the subsequent image processing.

As comparison criteria to OCT, we employed the diagnostic methods most widely used in dentistry: a clinical examination composed of visual and/or tactile inspection (shown in this paper by photographs) and a conventional X-ray. The dental X-Ray equipment used was the Spectro 70X (Dabi Atlante, Ribeirão Preto, São Paulo, Brazil), operating at 70 kVp head power and a head current of 8 mA. The radiographic film used was Kodak Dental Intraoral E-Speed Film (Carestream Health Inc., Rochester, New York, United States), and the dental developer and fixer, was from the same manufacturer.

During a clinical examination, it is possible to detect changes in resin composite color, polishing failures, contact point problems and major gaps and fissures; radiographic images can show excess or lack of restorative material, large areas of demineralization (typically greater than 30% of mineral loss), and gaps or fractures points larger than the minimum detection size observed by OCT. A well designed OCT system, on the other hand, is able to indicate micrometer sized external problems such as superficial cracks, and internal defects (air bubbles, cracks and their respective

growth, voids, gaps and fissures) as well as the characteristics of a specific composite material.

To evaluate the presence, or otherwise, of failures in the restorations, three experienced professionals, all of them Restorative Dentistry professors, were trained to interpret OCT images. Each professor was then individually shown the clinical photograph of each restoration in question, and requested to complete a form describing what they could see in that patient's image in terms of the restoration extension, and if there was any form of failure. In case of detected failure they were then asked to classify the failure. Then, the radiographic images were shown, in the same way and, last, the OCT images. To analyze the data a Kappa coefficient test was applied. Kappa coefficient is a statistical measure of the agreement for qualitative/categorical items; its aim is not to compare the diagnostic potential between the three techniques employed, but to compare how the evaluators agree among themselves in each form of diagnostic technique separately. After the analysis all of the patients that presented failures in their restorations were recalled to the clinic and had new procedures performed after a discussion with the patient following the approved clinical procedure.

Results

OCT images were obtained from vertical slices of the tooth, as indicated in figure 2. The scan was always mapped from left to right. The lateral distance between each image was 0.2 mm. For didactic reasons, we have only shown some tomograms of each tooth. The upper part of image corresponds to the cervical region and the lower part, the incisal region.

[Fig. 2]

Features seen in the OCT images were interpreted by reference to the literature and also to previous *ex vivo* studies by the authors, where the teeth were imaged via OCT and subsequently sectioned and histologically studied by light microscopy. It can be shown in figure 3, in which 3(a), 3(c), 3(e) and 3(g) represent OCT images of different samples restored in composite resin, and 3(b), 3(d), 3(f) and 3(h), their respective optical microscopy images. In figures 3(a) and 3(b) we can see an example of a well placed and sound restoration, whilst 3(c)/3(d) and 3(e)/3(f) show the air bubble presence (within the circle) close to the tooth restoration interface, as well as the dentin-enamel junction. The white appearance of the air bubbles in the optical microscopy images is due to the smear layer impregnation during the teeth sectioning with diamond wheel. Figures 3(g) and 3(h) show an aesthetic facet, in which is possible to observe the tooth-restoration limits (arrows), the dentin-enamel junction and, specially, the use of different shades of composite resin (large rectangles).

[Fig. 3]

Table 1 indicates a comparison between all the methods used in this work for the first three cases.

[Tab. 1]

Figure 4 shows a sequence of examinations of a patient with a well placed and sound restoration in a central incisor, placed seven years previously. Figure 4(a) represents the clinical examination; 4(b), the conventional radiograph showing the restoration at the incisal region in the circle. Arrows in 4(c) indicate the interface between the enamel and the restorative material, which can be clearly seen.

[Fig. 4]

Figure 5(a) shows a lateral incisor with an aesthetic facet (not polished) over an incisal and cervical restorations, confirmed by radiography in figure 5(b), performed

two weeks before the analysis reported here. In the OCT image, figure 5(b), an air bubble in the restoration (within the circle) can be seen and the dots indicate the points of microleakage at the enamel-restoration interface. The small rectangles indicate an extensive space under the restoration, probably due to resin polymerization contraction during the restorative procedure and the triangles indicate crack points between resin increments.

[Fig. 5]

Restorations involving medium and incisal regions of a central incisor, performed in 2001 in another patient are shown in figure 6, where Fig. 6(a) shows the clinical photograph with no sign of failure, and different colors between the resin composite and the dental enamel. In Fig. 6(b), the conventional radiograph, it is possible to observe excess restorative material at proximal surfaces; and Fig. 6(c) shows the OCT image sequence. The arrow here indicates the well placed enamel-restoration interface. However, several undesirable features can be identified: air bubble (within the circle); evidence of a gap between the enamel and the restorative material (identified by the dots); superficial defects and internal fractures in the resin composite (identified by the triangles).

[Fig. 6]

In some cases, a restoration does not necessarily need to present failures throughout its entire structure to be considered for replacement and they may well show one part which is well placed and intact whilst another area has problems. This can also be seen in figures 6(c) and 7. In the first slice of Fig. 6(c), we can see an arrow that indicates the well placed enamel-restoration interface, but in subsequent slices, we can see some failures, described previously. The same situation can be seen in figure 7, with a restoration involving medium and incisal regions. Arrows indicate the well placed

enamel-restoration interface; dots indicate enamel-restoration microleakages; triangles indicate evidence of superficial fissures at the resin composite; another feature is the different pseudo color of the resin composite at the incisal region when compared to medium region, marked with the large rectangles. This can be seen by OCT because lighter colors of resin have lower refractive indices, and thus this modifies the scattering in this region.

[Fig. 7]

In figure 8, we can see a sequence of failures over the entire structure of an incisal restoration (dots), beside the dentin-enamel junction.

[Fig. 8]

Finally, in figure 9, we can observe three different aesthetic facets. In the region indicated by the diamonds, problems with the cervical adaptation of the restorations are identified in Figs. 9(a) and 9(b), whereas a well suited adaptation is seen in Fig. 9 (c). None of these clinically important defects, seen by OCT, could be observed in the clinical images and X-rays, even when they were subsequently examined after the detecting a problem in the OCT data sets.

[Fig. 9]

Table 2 shows the Kappa coefficient results for each form of diagnostic examination. It can be seen that for clinical and radiographic examinations there was a substantial agreement between the evaluators, whilst for the OCT examinations the Kappa index obtained demonstrates perfect agreement: it means that the OCT images provide more accurate information to diagnostic than the clinical photographs and the X-ray exam. It was not possible to compare the kinds of failures seen in each type of examination, as the OCT is able to visualize internal structures that are impossible to be seen in the clinical inspection or radiographic examination.

[Tab. 2]

Discussion

The improvements in the esthetic and physical properties of composite resins over the past ten years have established them as the material of choice for restorations of anterior teeth when used in conjunction with the acid-etch technique and dental bonding systems [27]. However, their high aesthetic quality frequently makes it harder to see early signs of failure and due to the way that these materials behave, compared to traditional amalgam and gold restorations, early failure is more likely. Failures at the tooth-restoration interface can be associated with several factors including incorrect restorative technique, the physical properties of the materials used and, especially, the contraction of the material generated during the polymerization of the restorative material.

An adequate marginal adaptation and the integrity of the restoration are fundamental to the success of the dental treatment: failures in the marginal surface cause microleakage and bacteria infiltration; loss of integrity can be present in the internal or superficial structure of the restoration, and reduces the quality of the restoration, leading to early fracture of the restorative treatment. Some defects seen in this study are known to cause a loss of integrity in resin based composite restorations including air bubbles in the restoration, regions without material under the restoration (voids), cracks and fissures at the resin composite and gaps. When these kinds of failures are present and the restorative procedure is not adequate, a new treatment should be discussed with the patient.

Previous studies have shown some defects we have identified in this paper: the dentin enamel junction was evidenced by several authors [11, 12, 13]; Melo et al (2005) [15] presented induced marginal microleakage; Sadr et al (2009) [24] had shown the evolution of a marginal microleakage to a secondary caries with absence of restorative material under the restoration; the absence of restorative material in the interface between the restoration and the dental tissue (similar to that we have shown in figure 5), presence of gaps, as well as crack points of the restorative material were presented by Negritu et al (2009) [25]; air bubble and gaps were also presented in the study performed by Feldchtein et al (1998) [12] and, finally, crack propagation into the resin composite was described by Braz et al (2009) [17].

The current methods clinically used to diagnosis are not able to visualize micrometric structures. In the radiographic examination, for example, an early enamel caries lesion is visible only after approximately 30%–40% mineral loss [28]. This deficiency makes it difficult to diagnose early recurrent caries, when an earlier diagnosis means an easier and less traumatic treatment, leaving more enamel present in the tooth after treatment.

The Kappa coefficient was applied to analyze the concordance index of the diagnosis of the professionals selected for each examination modality separately, and the OCT method demonstrated perfect agreement between the evaluators, while there was a substantial agreement for the clinical and radiographic examinations. This indicates that OCT, besides be a good tool for diagnosis can be consistently interpreted by well trained dentists. However, it was not possible to use a statistical test to compare the clinical, X-ray and OCT examinations simultaneously. The first method (clinical observation) is only able to see defects at external surfaces; radiographic methods image across the tooth, but the resulting image inherently overlays the buccal and lingual

surfaces making it difficult to detect and determine internal problems. OCT can produce two dimensional and cross-sectional images, allowing the observer to see external and internal details, without overlap of structures, being able to accurately locate the visualized structures. Thus teeth were visualized in different forms in each type of examination, but many of the minor defects (air bubbles, for example) only can be seen by OCT. However, all defects detected by clinical and X-ray examinations were also detected using the OCT protocol.

This study demonstrates that OCT is a powerful tool for the early detection of failures on restorations, through visualization of microleakages, internal fractures, superficial cracks and fissures, tooth demineralization under the restorative material and cervical adaptation of the restorations. Incipient lesions can be precisely located, their depth may be measured and their proximity to the dentin-enamel junction may be determined. The sensitivity of the OCT technique is sufficient such that details, including the use of different colors of resin composite used to increase the esthetic aspect of a restoration, can be identified due to the slightly different scattering properties (see figure 7).

As dentists are used to dental radiographs for diagnostic purposes, OCT imaging, which shows similar dental morphology, could be readily adopted [4] and, ideally, the number of conventional X-ray investigations would be reduced in order to minimize the patients exposure to ionizing radiation [13].

However, it is necessary to recognize some limitations of OCT: the system has a small depth penetration, (1-3 mm in teeth), which is, however, adequate for enamel and even dentin visualization. This is partly because we chose to use light at 850nm in order to increase the contrast between areas with only slightly different scattering properties. The use of longer wavelength sources (around 1300nm), with some slight loss of

contrast, and hence sensitivity, may provide the best compromise between depth of imaging and sensitivity to minor alterations in structure. Furthermore, our current system does not allow the use of the technique in every tooth, just on incisors and canines. Thus for this first stage of our studies applying OCT *in vivo*, we only assessed anterior teeth, for two reasons: incisors and canines are the teeth that require better esthetic restorative procedures, and the unavailability of a handpiece probe, presently under development, to reach the posterior dentition.

The time acquisition for each image is less than one second; so considering that we performed one image at every 0.2 mm, and including the time to save the images, the complete examination takes between 2-4 minutes, depending of the tooth width.

Some difficulties were found during the data collection of this study: the major of them was to control the production of saliva and subsequent patient movement, which tended to produce image artifacts. Thus was minimized by careful explanation to the patient and the use of the stabilization bar. A further complication was to undertake the examinations in patients presenting a maxillary overjet (an orthodontic condition in which the third incisor is ahead of the cervical third in the upper incisors, and thus the teeth appear to be inclined horizontally) – this problem was solved by requesting the patient to bow their head slightly but, in a long term, the solution is in the development of a handpiece probe.

The software in the current system does not permit the construction of volumetric three dimensional imaging generation that could present interesting visual effects and might provide the clinician, in the longer term, with novel and potentially useful views of the tooth. This is an area for future study and here we have presented the data in a manner which is familiar to the dental practitioner, as a 2 dimensional data set, though their experience of X-rays.

Further clinical studies covering cervical adaptation of aesthetics-facets and fixed crowns are currently underway. The high sensitivity of OCT to minor defects also opens up a further clinical question over which minor defects will progress to server complications and which may stay at the minor level. The development of such revised treatment protocols is beyond the scope of the present study but it is an area that will need to be investigated as OCT moves towards a standard diagnostic instrument in clinical practice, as is the case with any new technological advance.

Conclusions

Compared to conventional radiography, OCT is a powerful tool for investigation of failures at the tooth-restoration interface. OCT is able to exactly visualize external and internal micrometric structures, not perceived by clinical examination or conventional radiography, proving its superiority as a technique for early diagnosis of restoration failures and prevention of recurrent caries. However, because of the low penetration depth of OCT, conventional radiography imaging may not be totally substituted. This was a qualitative study applying OCT in dental clinics; we used conventional X-Ray, the most widely used modality of imaging for diagnostic assessment in dental clinics, and the clinical examination as the comparison for our study. We analyzed the differences between the modalities of exams mentioned above and the advantages and limitations of conventional radiography and OCT examinations. Besides other applications of the OCT technique *in vivo*, further complementary studies are under-way to determine dental composites failures in a quantitative manner, as well as their size or extent.

Acknowledgements

The authors are thankful to the Prosthetics and Buco Facial Surgery Department at Universidade Federal de Pernambuco, especially to the Professors Lúcia Beatrice, for loaning us space to set up the OCT equipment in the Faculty of Dentistry, and to Adolfo Cabral and Paulo Fonseca, to allow the selection of patients at the clinics under their responsibility. Financial support of this work from CNPq, FACEPE (under the PRONEX program supporting the Center of Excellence in Nanophotonics and Biophotonics) and CAPES, Brazilian Agencies, are gratefully acknowledged. This work was part of the MSc dissertation of Cláudia C. B. O. Mota.

References

[1] A. Hall and J. M. Girkin, "A review of potential new diagnostic modalities for caries lesions," *Journal of Dental Research* **83** Spec C:C89–94 (2004).

[2] D. Fried, J. D. Featherstone, C. L. Darling, R. S. Jones, P. Ngaotheppitak and C. M. Buhler, "Early caries imaging and monitoring with near-infrared light," *Dent. Clin. North. Am.* **49**(4), 771–93 (2005).

[3] A. C. Ko, L. P. Choo-Smith, M. Hewko, L. Leonardi, M. G. Sowa, C. C. Dong, P. Willians and B. Gleghorn, "Ex vivo detection and characterization of early dental caries by optical coherence tomography and Raman spectroscopy," *J. Biomed. Opt.* **10**(3), 0311182005.

[4] L. P. Choo-Smith, C. C. S. Dong, B. Cheghorn and M. Hewko, “Shedding new light on early caries detection,” *JCDA* **74**(10), 913-918 (2009).

[5] D. Huang, E. A. Swanson, C. P. Lin, J. S. Schuman; W. G. Stinson; W. Changw; M. R. Hee; T. Flitte; K. Gregory; C. A. Puliafito and J. G. Fujimoto, “Optical coherence tomography,” *Science* **254**, 1178-1181 (1991).

[6] B. E. Bouma, G. J. Tearney and B. Bouma, *Handbook of Optical Coherence Tomography*, Marcel Dekker (2002).

[7] M. C. Pierce, J. Strasswimmer, B. H. Park, B. Cense and J. F. de Boer, “Advances in optical coherence tomography imaging for dermatology,” *The Jounal of Investigative Dermatology* **123**, 458-463 (2004).

[8] G. J. Tearney, S. A. Boppart, B. E. Bouma, M. E. Brezinski, N. J. Weissman, J. F. Southern and J. G. Fujimoto, “Scanning single-mode fiber optic catheter-endoscope for optical coherence tomography,” *Opt. Lett*. **21,** 543-545 (1996).

[9] S. A. Boppart, G. J. Tearney, B. E. Bouma, J. F. Southern, M. E. Brezinski and J. G. Fujimoto, "Noninvasive assessment of the developing Xenopus cardiovascular system using optical coherence tomography," *Proc. Natl. Acad. Sci.* **94**, 4256-4261 (1997).

[10] Y. Yang, A. Dubois, X. Qin, J. Li, A. E. Haj and R. K. Wang, “Investigation of optical coherence tomography as an imaging modality in tissue engineering,” *Phys. Med. Biol*. **51**, 1649-1659 (2006).

[11] B. W. Colston, U. S. Sathyam, L. B. Da Silva, M. J. Everett, P. Stroeve and L. L. Otis, "Dental OCT." *Opt. Express* **3**(6), 230-238 (1998).

[12] F. I. Feldchtein, G. V. Gelikonov, V. M. Gelikonov, R. R. Iksanov, R. V. Kuranov, A. M. Sergeev, N. D. Gladkova, M. N. Ourutina, J. A. Warren and D. H. Reitze, "In vivo OCT imaging of hard and soft tissue of the oral cavity," *Opt. Express* **3**(6), 239–250 (1998).

[13] R. Brandenburg, B. Haller and C. Hauger, "Real-time in vivo imaging of dental tissue by means of optical coherence tomography (OCT)," *Optics Communications* **227**, 203-211 (2003).

[14] W. Jung, J. Zhang, J. Chung, P. Wilder-Smith, M. Brenner, J. S. Nelson and Z. Chen, "Advances in oral cancer detection using optical coherence tomography," *IEEE J. Select. Topics Quantum Electron.* **11**(4), 811-817 (2005).

[15] L. S. A. de Melo, R. E. de Araujo, A Z Freitas, D. Zezell, N D. Vieira Jr , J. Girkin, A. Hall, M. T Carvalho and A. S. L. Gomes, "Evaluation of Enamel Dental Restoration Interface by Optical Coherence Tomography," *J. of Biomedical Optics* **10**(6), 064027-1/5 (2005).

[16] A. Z. Freitas, D. M. Zezell, N. D. Vieira Jr., A. C. Ribeiro and A. S. L.Gomes, "Imaging carious human dental tissue with optical coherence tomography," *J. of Appl. Phys.* **99**, 024906/1-6 (2006).

[17] A. K. Braz, B. B. Kyotoku, R. Braz and A. S. L. Gomes, "Evaluation of crack propagation in dental composites by optical coherence tomography," *Dent. Mater*. **25**, 74-79 (2009).

[18] C. M. F. Kauffman, M. T. Carvalho, R. E. Araújo, A. Z. Freitas, D. M. Zezell and A. S. L. Gomes, "Characterization of the dental pulp using optical coherence tomography," *Proceedings of the SPIE* **6137**, 51-58 (2006).

[19] D. D. Fonseca, B. B. C. Kyotoku, A. M. A. Maia and A. S. L. Gomes, "In vitro imaging of remaining dentin and pulp chamber by optical coherence tomography: comparison between 850 and 1280 nm," *Journal of Biomedical Optics* **14**(2), 024009 (2009).

[20] H. Shemesh, G. van Soest, M. K. Wu, L. W. M. van der Sluis and P. R. Wesselink, "The Ability of Optical Coherence Tomography to Characterize the Root Canal Walls," *JOE* **33**(11), 1369-1373 (2007).

[21] C. Sinescu, M. L. Negritu, S. Antonie, G. Dobre, A. Bradu, M. Hughes, M. Rominu and A. G. Podoleanu, "Marginal adaptation analysis performed with en face optical coherence tomography in fixed partial dentures," *Proc SPIE* **7258**, 72584H (2009).

[22] N. Attar, Y. Korkmaz, E. Ozel, C. O. Bicer and E. Tiratli, "Microleakage of class V cavities with different adhesive systems prepared by a diamond instrument and different

parameters of Er:YAG lasers irradiation," *Photomedicine and Laser Surgery* **26**(6), 585-591 (2008).

[23] H. Xie, F. Zhang, Y. Wu, C. Chen and W. Liu, "Dentine bond strength and microleakage of flowable composite, compomer and glass ionomer cement," *Australian Dental Journal* **53**, 325-331 (2008).

[24] A. Sadr, J. Tagami, Y. Shimada and Y. Sumi, "Optical coherence tomography for in vivo assessment of class-III composite restoration," *Journal of Dental Research* **88** (Spec Iss A): 1106 (2009).

[25] M. L. Negritu, C. Sinescu, M. Rominu, M. Hughes, G. Dobre and A. G. Podoleanu, "Optical coherence tomography and confocal microscopy investigations of dental structures and restorative materials," *Proc. SPIE* **7258**, 72584N (2009).

[26] M. Wojtkowski, A. Kowalczyk, R. Leitgeb and A. F. Fercher, "Full range complex spectral optical coherence tomography technique in eye imaging," *Optics Letters* **27**, 1415-1417 (2002).

[27] S. K. Garoushi, L. V. J. Lassila and P. K. Vallittu, "Fatigue strength of fragmented incisal edges restored with a fiber reinforced restorative material," *The Journal of Contemporary Dental Practice.* **8**(2), 1-10 (2007).

[28] S. C. White and M. J. Pharoah. "Dental caries," in *Oral radiology: principles and interpretation*. 5th ed. Toronto: Mosby; 2004. p. 297–313.

Figure Captions

Figure 1. OCT setup. 1(a) schematic diagram of SD-OCT, operating at 850nm; 1(b) dental SD-OCT adapted for *in vivo* study; 1(c) positioning of patient.

Figure 2. Sequence indicating the scan positioning in the patient's teeth, identifying the tomographic slices.

Figure 3. OCT and their respective optical microscopy images of different samples restored with resin composite. In 3(a) and 3(b), arrows indicate the well suited restoration, whilst in 3(c)/3(d) and 3(e)/3(f) air bubble close to the tooth restoration interface can be seen within the circles; in DEJ, we can observe the dentin-enamel junction; 3(g) and 3(h) show an aesthetic facet, in which is possible to observe the tooth-restoration limits (arrows) and the use of different shades of composite resin (large rectangles). Red bar represents 1 mm.

Figure 4. Well suited restoration of a central incisor. 4(a) clinical photograph; 4(b) conventional radiography; 4(c) sequence of OCT images: arrows indicate the integrity in the enamel-restoration interface. Red bar represents 1 mm.

Figure 5. An aesthetic facet over an incisal restoration. 5(a) clinical photograph; 5(b) conventional radiography; 5(c) sequence of OCT images: air bubble (shown within the major circle); gaps at the interface enamel-restoration (indicated by the dots); small rectangles indicate an space under the restoration, probably due to polymerization

contraction; and the triangles, crack points between resin increments. Red bar represents 1 mm.

Figure 6. Restoration involving medium and incisal regions. 6(a) clinical photograph; 6(b) conventional radiography; 6(c) sequence of OCT images: arrow indicates the well suited enamel-restoration interface; within the circle, an air bubble; dots indicate gaps at the enamel-restoration interface; triangles shows superficial defects and internal fractures at the resin composite; stars indicate imaging artifacts. Red bar represents 1 mm.

Figure 7. Restoration involving medium and incisal regions. Arrows indicate the well suited enamel-restoration interface; dots, the presence of gaps; triangles demonstrate superficial fissures at resin composite; within the large rectangle, we can observe a darker region, corresponding to lighter resin color increment in the incisal part of restoration. Red bar represents 1 mm.

Figure 8. Sequence of an incisal restoration with defects throughout the entire structure. Dots indicate gaps between the restorative material and the dental enamel; in DEJ, we can observe the dentin-enamel junction; artifact imaging indicated by star. Red bar represents 1 mm.

Figure 9. Three different aesthetic facets. Diamonds indicate problems with cervical adaptation of the restorations in 9(a) and 9(b), and a well suited adaptation in 9(c). Red bars represent 1 mm.

Table caption

Table 1. A summary of the preliminary results.

Table 2. Kappa coefficient results.

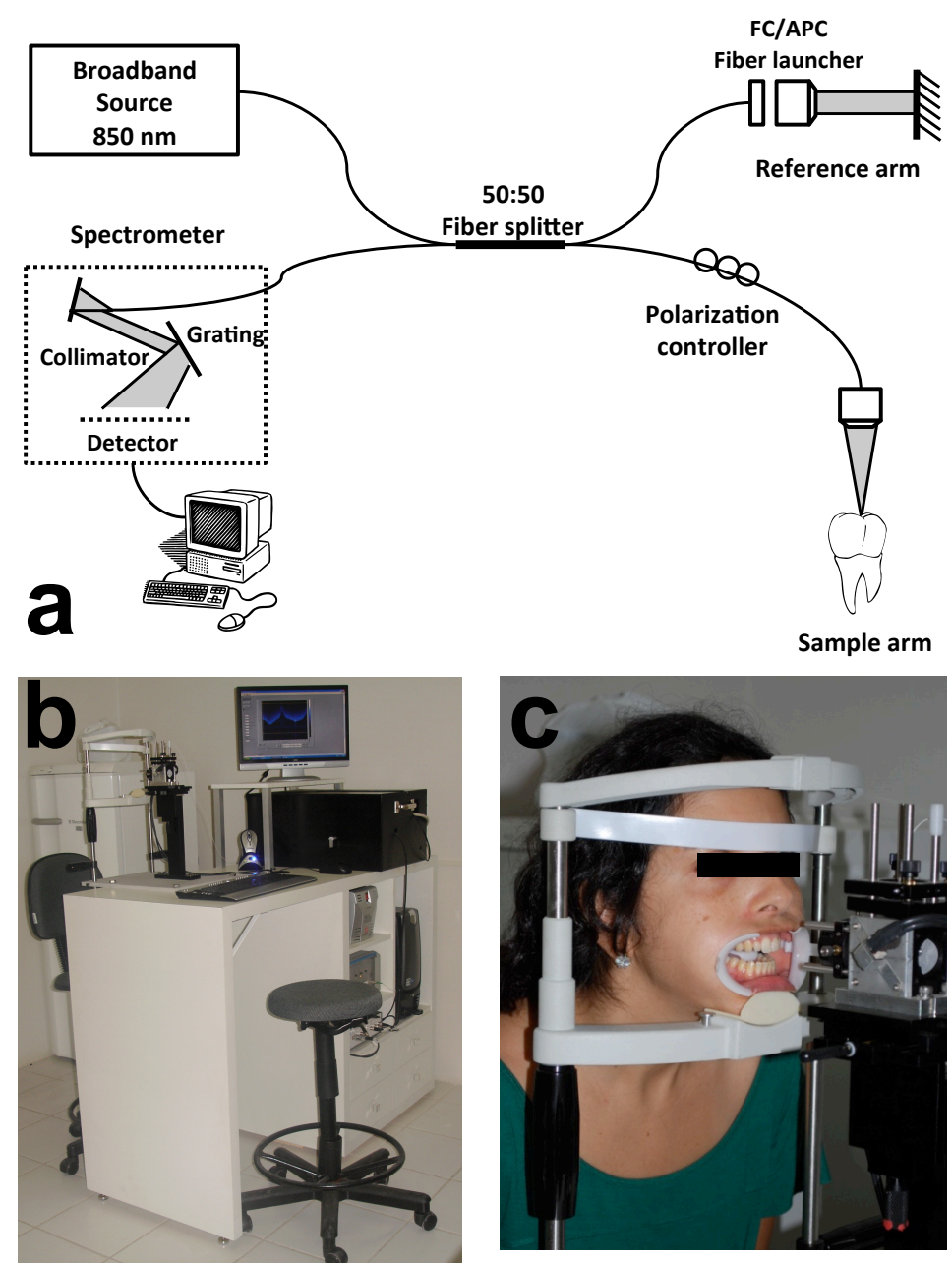
Broadband
Source
850 nm
FC/APC
Fiber launcher
Reference arm
50:50
Fiber splitter
Spectrometer
Collimator
Grating
Detector
Polarization
controller
Sample arm
a
b
c

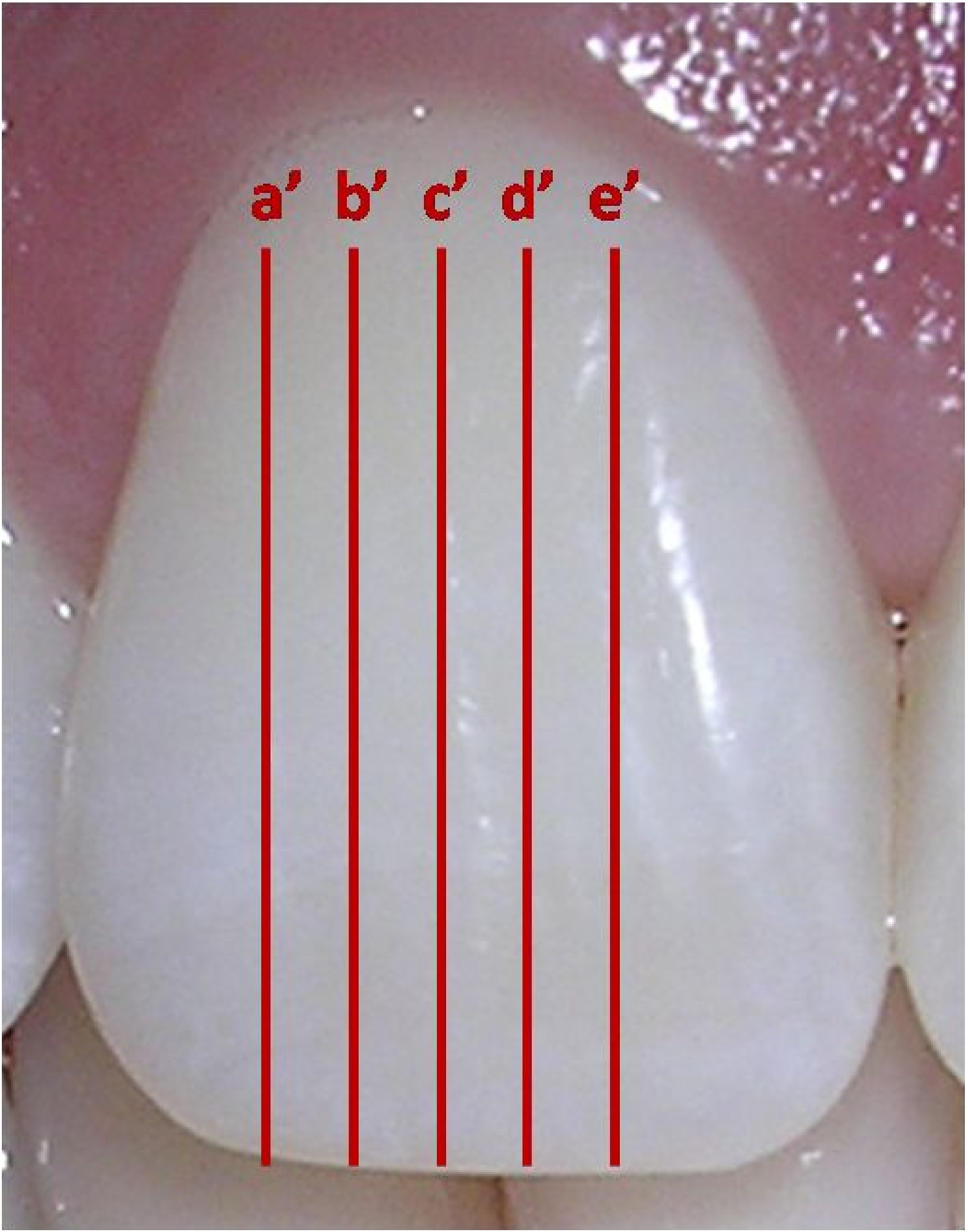
a’
b’
c’
d’
e’

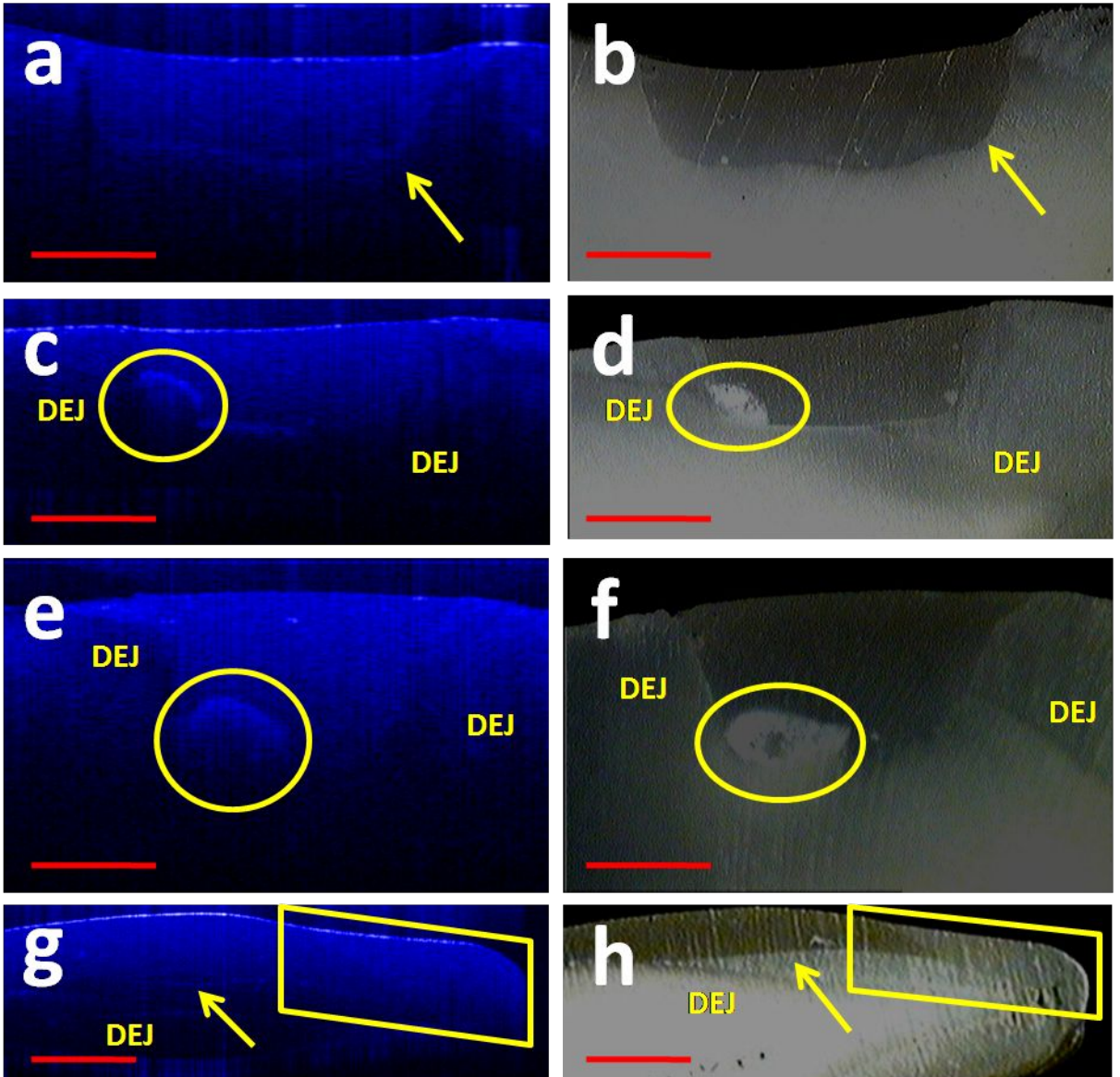
a
b
c
DEJ
DEJ
d
DEJ
DEJ
e
DEJ
DEJ
f
DEJ
DEJ
g
DEJ
h
DEJ

Patient Number	Visual inspection defect	X-ray exam defect	OCT defect	Comment
1	No	No	No	A well placed and sound restoration (Fig. 4)
2	No	No	Yes	From a visual inspection, is only possible to observe that the restoration is not polished (Fig. 5)
3	No	Yes	Yes	X-ray exam only shows the excess of restorative material, but is not able to visualize the failures seen by OCT (Fig. 6)

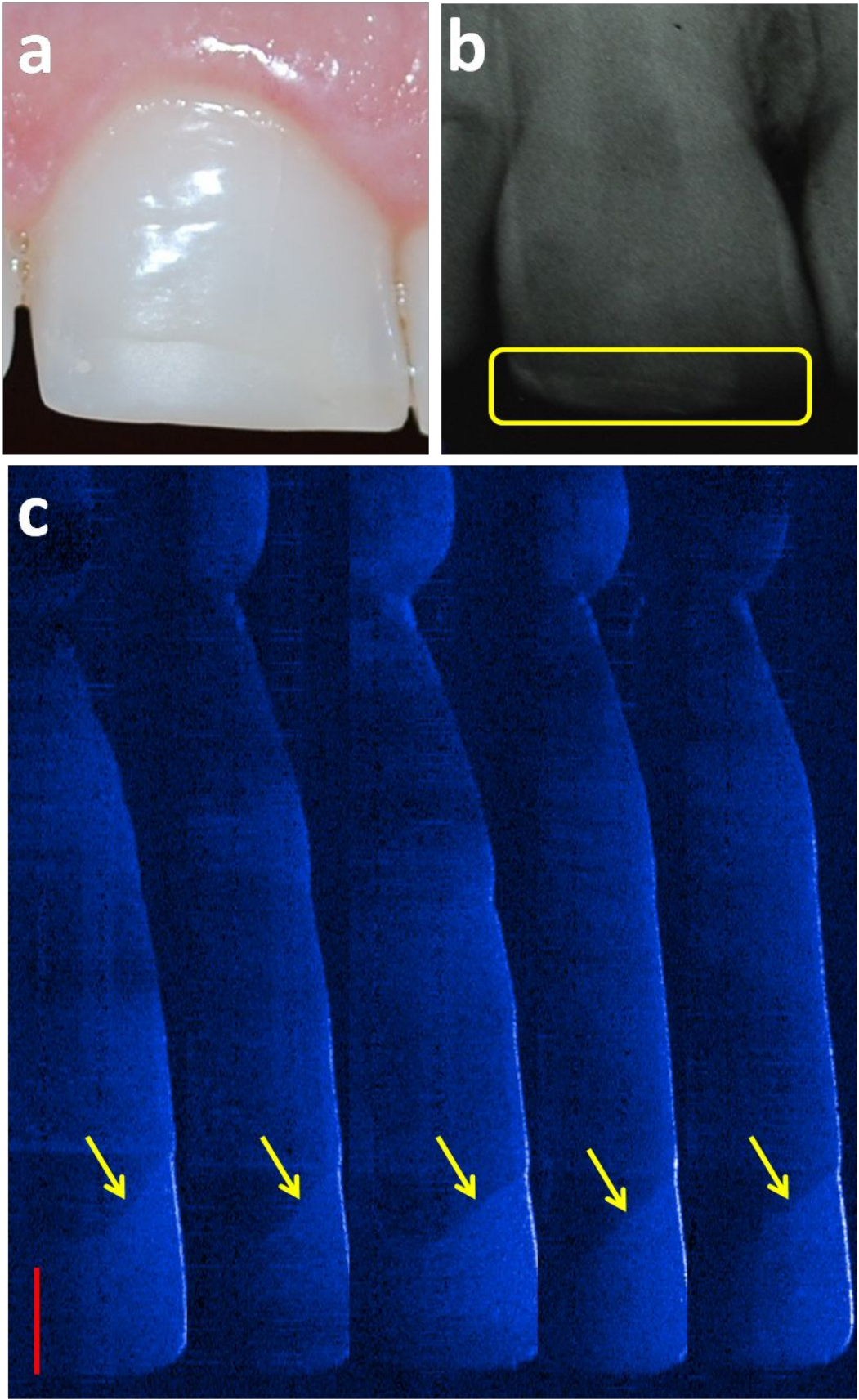
a
b
c

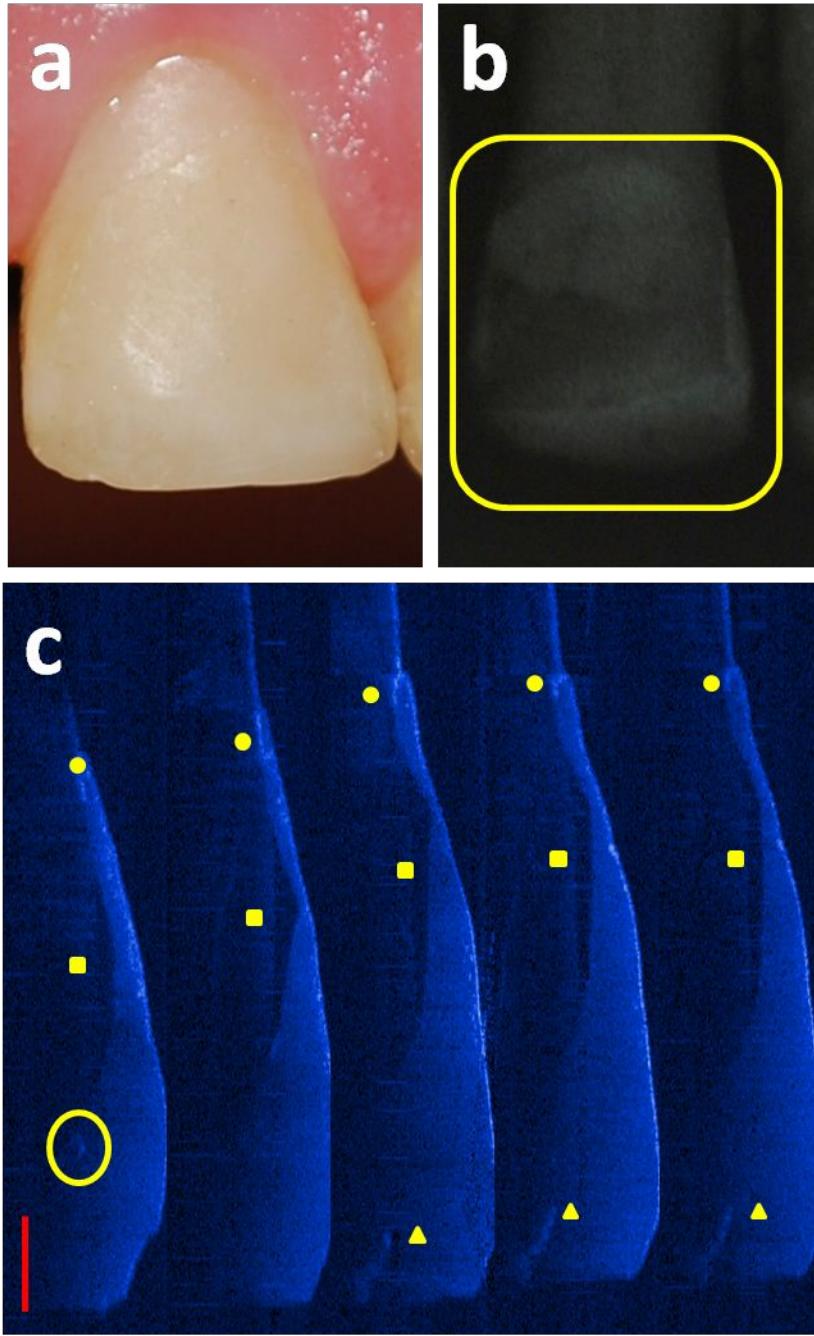
a
b
c

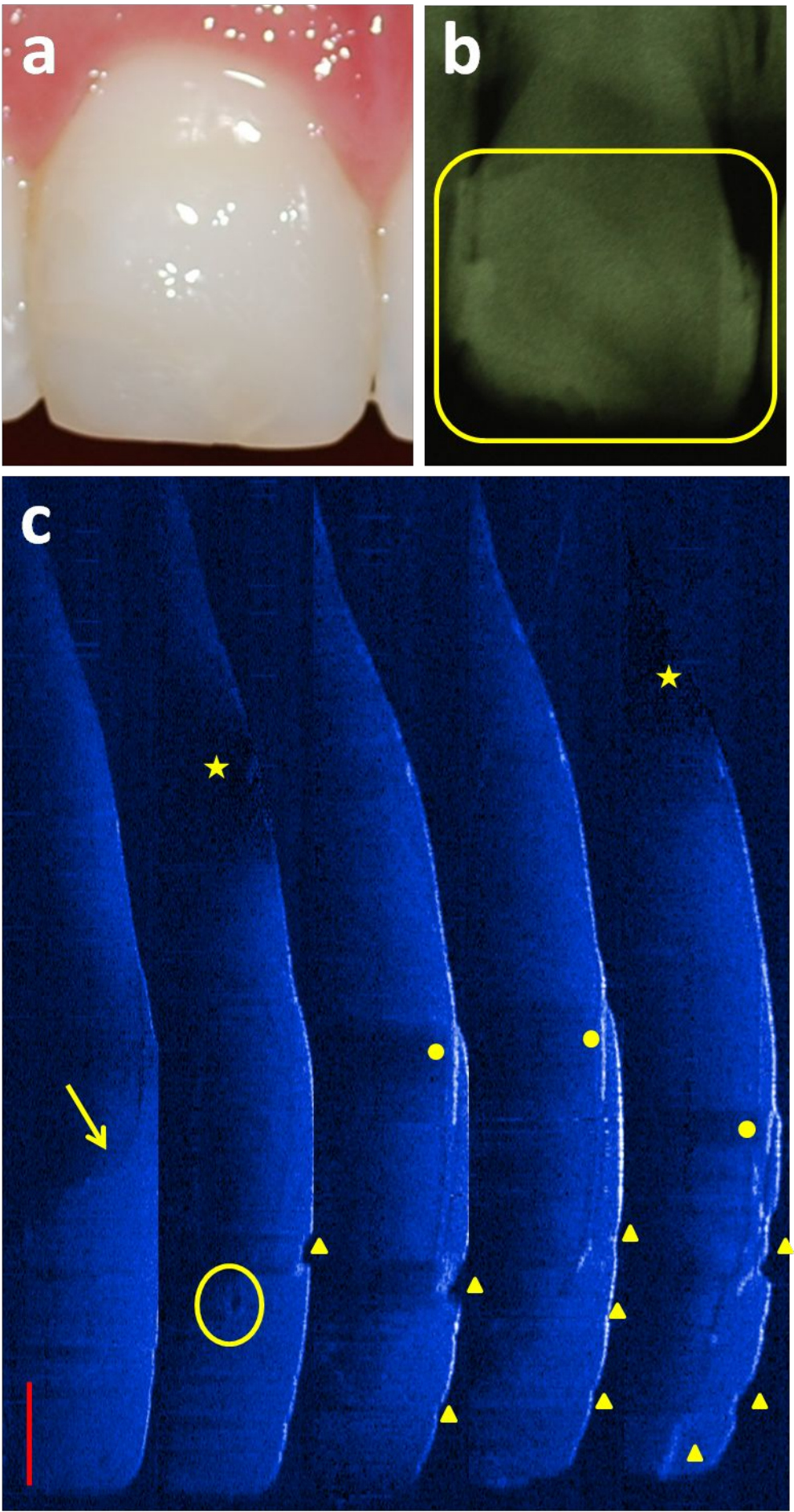
a
b
c

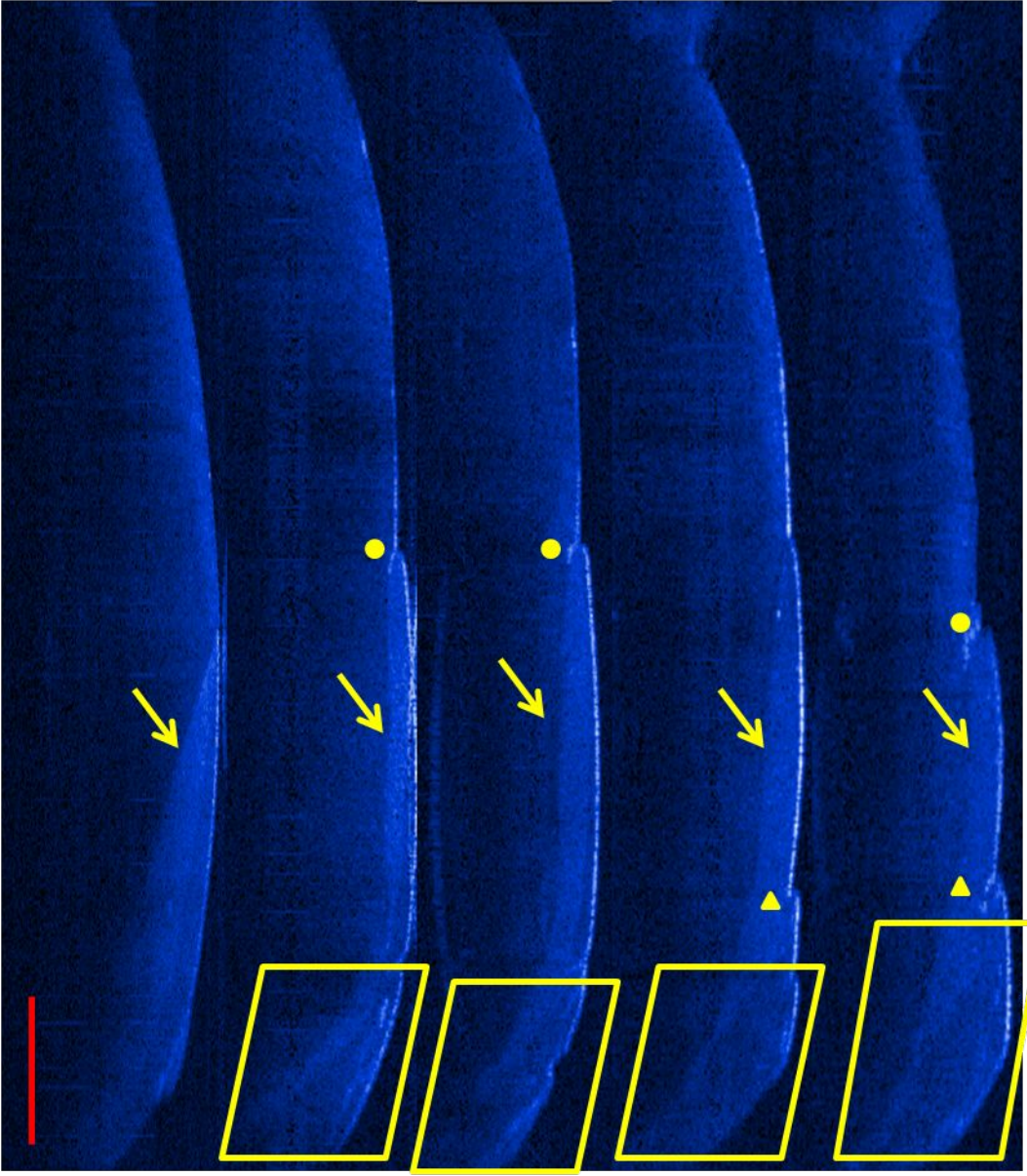

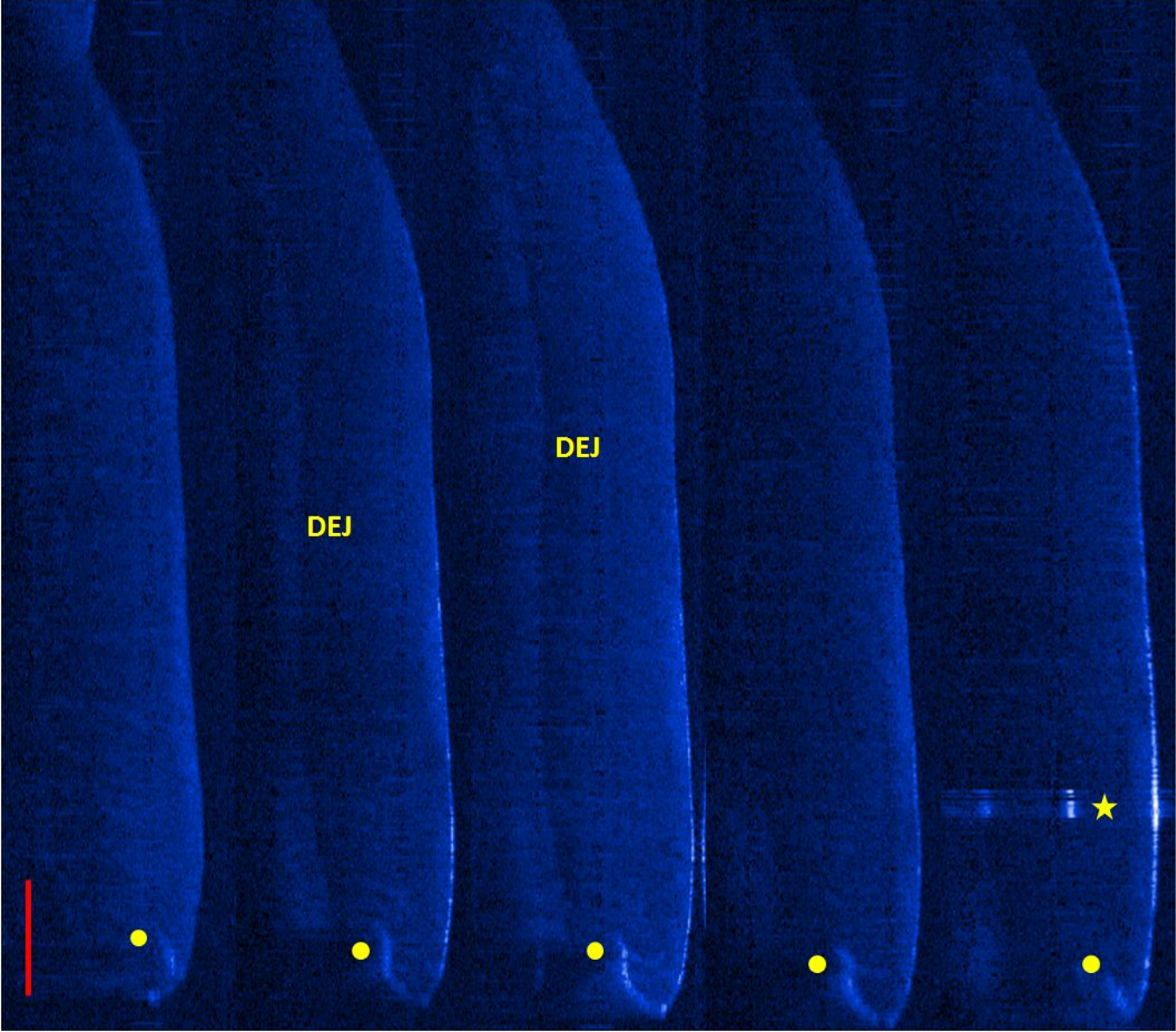
DEJ
DEJ

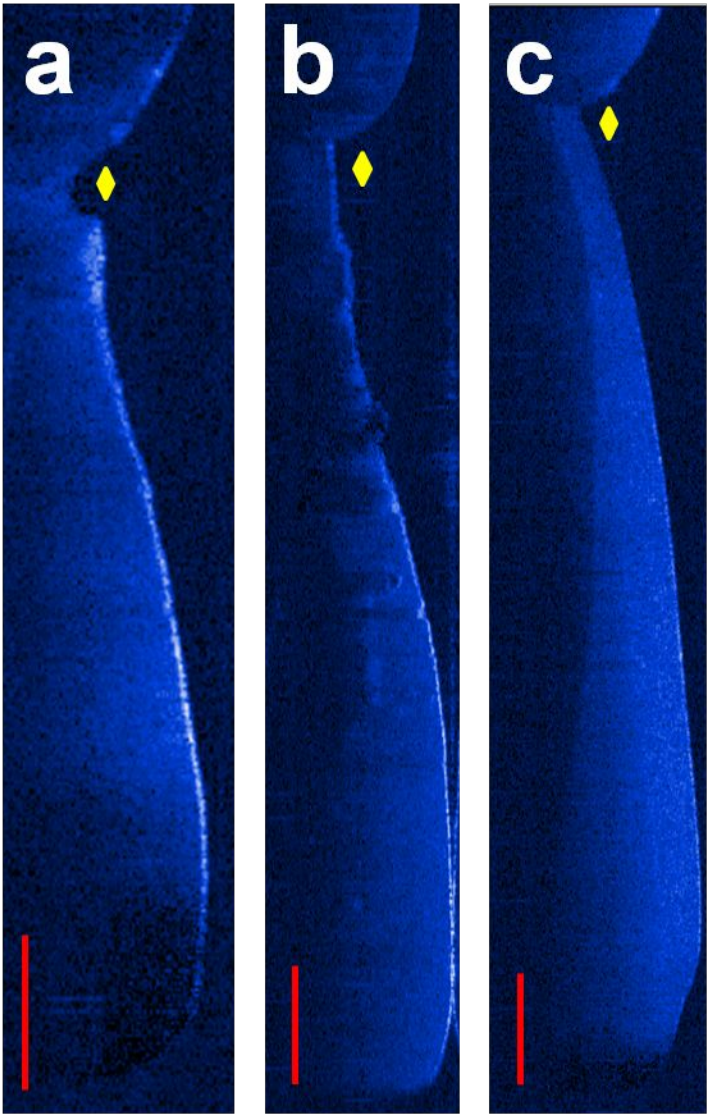
a
b
c

	Clinical exam	Radiographic exam	OCT
Kappa	0,732	0,732	1,000
p-value	< 0,001	< 0,001	< 0,001
Kappa 95% range trust	**Upper:** 1,000 **Lower:** 0,374	**Upper:** 1,000 **Lower:** 0,374	**Upper:** 1,000 **Lower:** 0,642